

# Eyes on VLM: Benchmarking Gaze Following and Social Gaze Prediction in Vision Language Models

Hengfei Wang\* Anshul Gupta\* Pierre Vuillecard Jean-Marc Odobez  
Idiap Research Institute

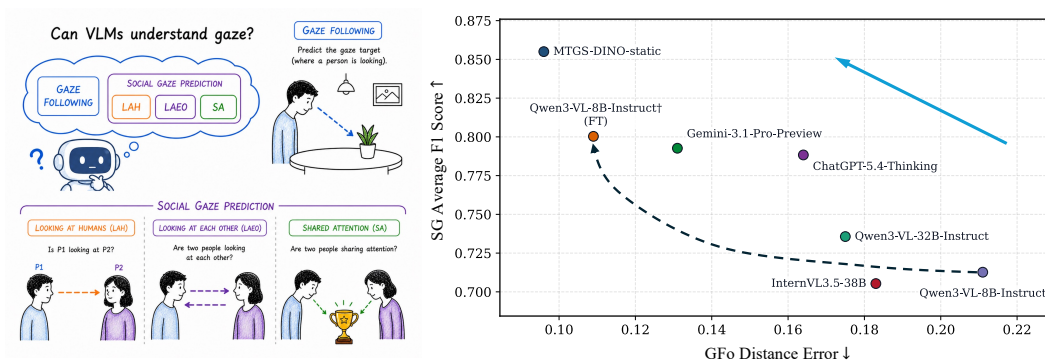


Figure 1: **EyeVLM overview.** Left: Gaze Following (GfO) and Social Gaze Prediction (SG). Right: model comparison on GazeFollow [1] (GfO distance error ↓) and VideoAttentionTarget [2] (SG F1 ↑). Results are taken from Table 4. Fine-tuning (FT) improves VLMs over dedicated prompting, but they still lag behind specialized pure vision gaze models.

## Abstract

Vision-language models (VLMs) have rapidly evolved into general-purpose multi-modal reasoners with strong zero-shot generalization. In this context, VLMs could greatly benefit the analysis of human gaze and attention, a central task in human behavior understanding that requires reasoning about the physical scene as well as the activity, interactions, and social context. However, the extent to which VLMs can reliably understand human gaze and related attentional behaviors remains largely unexplored. In this work, we present **EyeVLM**, a systematic evaluation framework for *gaze understanding* in VLMs across two complementary dimensions: *tasks* and *models*. To assess gaze understanding capabilities, we focus on two core tasks. The first, **gaze following**, i.e. predicting the 2D location where a person is looking at, has a geometric and visual processing focus, requiring precise understanding of the human face, attention direction, 3D scene structure and spatial grounding of attended targets. The second, **social gaze prediction**, requires social and relational reasoning over multi-person interactions (e.g., mutual gaze and shared attention), and may benefit more from the LLM semantic reasoning capabilities within VLMs. Regarding models, **EyeVLM** evaluates these tasks in two ways: a zero-shot setting with a diverse set of state-of-the-art open- and closed-source VLMs, exploring different prompting strategies; and a fine-tuning approach based on task-specific QA pairs, studying the impact of *model scale* and *data scale*. As benchmarks, we rely on existing gaze understanding datasets and perform a systematic comparison with state-of-the-art purely visual models. Overall, our results show that current VLMs lack precise gaze understanding capabilities. While standard training helps reduce the gap with visual models, significant improvements are still needed.

\*Equal contribution.

# 1 Introduction

Understanding gaze is a key component of social cognition, as it provides direct cues about others’ attention and underlying intent [3, 4]. It plays a central role in non-verbal communication, supporting the inference of intentions, the regulation of interactions, and the establishment of joint attention [5]. Accurate gaze understanding is therefore essential for modeling social behavior and reasoning about interactions and social context.

In computer vision, human gaze understanding has been extensively studied through dedicated tasks such as 3D gaze estimation, gaze following, and social gaze prediction. Gaze following aims to infer a person’s attended target in the scene, typically represented as a 2D point or heatmap. Social gaze prediction focuses on interaction-level phenomena, including mutual gaze (LAEO) [6], looking-at-person behaviors (LAH) [7], and shared attention (SA) [8] in multi-person settings. Over the past decade, the field has developed benchmarks and specialized models for these tasks, evolving from early convolutional approaches [1, 2] to more recent transformer-based [4] and unified frameworks, including multi-person [9] and temporal models [10], as well as methods incorporating 3D scene representations for improved geometric reasoning.

Despite these advances, it remains unclear to what extent current models achieve true scene understanding. In particular, gaze reasoning requires situated perception, including understanding the person’s activity, modeling interactions with objects or other individuals, and grounding predictions in 3D space. Without such capabilities, generalization and further performance improvements may be limited, and the gap to human-level understanding may persist.

In contrast, vision–language models (VLMs) have recently emerged as general-purpose multimodal reasoners, demonstrating strong zero-shot and few-shot transfer across diverse visual understanding tasks [11–13]. Powered by large-scale pretraining and instruction tuning, modern VLMs can parse complex scenes, capture high-level semantics, and leverage linguistic knowledge about social interactions and human behavior. This suggests that VLMs may be particularly well suited to address the limitations of specialized gaze models, especially for tasks requiring social reasoning and contextual understanding.

This shift raises a key question: to what extent do VLMs understand human gaze, a fundamental social and perceptual signal underlying attention, communication, and interaction? More broadly, the adoption of VLMs moves the paradigm from task-specific architectures to generalist models guided by prompting and lightweight adaptation, raising the question of whether gaze understanding can be addressed within this framework. However, despite the maturity of gaze-following and social gaze prediction research, a systematic evaluation of modern VLMs on these tasks is still lacking. In particular, we lack a unified study covering (i) diverse gaze tasks and datasets, (ii) a representative set of open and closed-source models under consistent protocols, (iii) the impact of prompting and adaptation strategies, and (iv) fair comparisons with state-of-the-art pure visual models. Existing gaze literature focuses on specialized models, while VLM behavioral studies rarely isolate gaze as a standalone capability, instead treating it implicitly within broader visual reasoning tasks [14, 15]. As a result, it remains unclear what VLMs can achieve out of the box, when and why they fail, and how they should be effectively prompted or adapted for gaze understanding.

To address this gap, we introduce **EyeVLM**, an evaluation framework designed to systematically assess gaze understanding in VLMs. It is organized along two main dimensions: tasks and models.

First, at the task level, we study two representative problems: gaze following and social gaze prediction, which exhibit different scene understanding requirements. Gaze following relies on gaze direction perception, 3D scene structure, and geometric reasoning to localize attended targets within a situated context (e.g., activity, gestures). In contrast, social gaze prediction emphasizes relational reasoning over multi-person interactions, such as predicting gaze relationships between individuals. EyeVLM standardizes task interfaces so they can be queried through language and enables direct comparison with state-of-the-art visual models.

Second, at the model level, we conduct zero-shot evaluations of a diverse set of state-of-the-art VLMs, including both open and closed-source models. We study multiple prompting strategies (Chain-of-Thought, In-Context learning), including variations in instruction templates and reasoning cues. Given the subtle visual and relational nature of gaze understanding, prompt design is expected to significantly influence both task interpretation and output structure. Beyond zero-shot evaluation, EyeVLM also probes adaptability. We construct task-specific QA pairs for supervised fine-tuning

and adapt representative open VLM families (Qwen [16]) to assess how fine-tuning affects gaze understanding. We further analyze the impact of using multiple datasets or tasks during training.

**EyeVLM** is designed as a diagnostic tool. By jointly analyzing results across tasks, models, and prompting strategies, we aim to characterize the current capabilities and limitations of VLMs for gaze understanding. In summary, our main contributions are threefold:

- A unified benchmark for gaze understanding in VLMs. We introduce **EyeVLM**, covering gaze following and social gaze prediction with standardized language-based interfaces and comparison to vision-based models.
- Analysis of zero-shot performance and prompting. We evaluate diverse VLMs and study the impact of prompting strategies (Chain-of-Thought, In-Context) on gaze understanding.
- Study of fine-tuning. We construct QA pairs for adaptation and analyze how fine-tuning, model scale, and data scale influence performance.

## 2 Related Work

**Gaze Following** Typical approaches to gaze following adopt a two-branch architecture: one branch analyzes the broader scene to identify salient objects or regions, while the other analyzes the head of the person of interest to estimate gaze direction. Information from the two branches is then fused to produce the final prediction [1, 17, 2, 18–21]. Subsequent work has shown the benefits of incorporating additional modalities, such as scene depth [17, 19, 21] and human pose [19]. Other studies further explored temporal modeling [2, 22] but have shown limited improvements. Additionally, multi-person transformer based architectures have enabled single-pass prediction for multiple individuals [9, 10]. Most recently, Gaze-LLE leveraged large-scale learned visual encoders with lightweight decoding to reach strong performance, highlighting the value of foundation representations for gaze [4]. However, these advances largely assume task-specific training and outputs, motivating EyeVLM to systematically evaluate how general-purpose VLMs handle gaze following under varying models, prompts, and adaptation settings.

**Social Gaze Prediction** Early work formulated mutual gaze detection in unconstrained videos using head pose and geometry cues [23]. LAEO-Net and LAEO-Net++ introduced track-based spatiotemporal deep models to improve robustness beyond frame-wise decisions [24, 6], and were followed by other deep learning based models [25, 26]. Fan et al. [8] introduced a model for in-the-wild shared attention estimation by combining gaze cones from individuals with object region proposals in the scene. Attention Flow learns shared attention end-to-end, highlighting the benefit of modeling collective focus rather than post-processing individual gaze [27]. More recent unified formulations jointly predict gaze targets and social gaze labels [7], and temporal multi-person frameworks further connect gaze following with social gaze prediction at scale [10]. However, existing methods remain specialized and dataset-dependent, motivating EyeVLM to systematically evaluate VLMs on social gaze prediction across model families, prompt strategies, and fine-tuning/data scaling.

**Vision-Language Models** Vision-language models (VLMs) have shown strong generalization across visual reasoning tasks through large-scale image-text pretraining and instruction tuning [11–13]. However, gaze understanding remains a fine-grained and socially grounded capability that is rarely isolated in standard VLM benchmarks. Recent studies have begun to explore the connection between VLMs and gaze understanding. Gupta et al. [28] use VLMs as zero-shot contextual cue extractors and inject the predicted cues into a specialized gaze following model. GazeLLM [29] employs a pretrained LLM to perform spatial-semantic reasoning over structured object representations, improving specialized vision gaze following architecture through a plug-and-play fusion module. GazeVLM [30] develops a dedicated VLM for multi-task gaze understanding with RGB, depth, and textual prompts. Despite these efforts, existing works mainly use VLMs as auxiliary modules, construct gaze-specific VLMs, or improve specialized gaze models through language reasoning. A recent exception is VL4Gaze [31], which formulates gaze following as a VQA-style problem and constructs a multi-task benchmark covering gaze description, localization, and ambiguity recognition.

However, none of these works consider social gaze prediction. Furthermore, none of them do a systematic comparison between current general-purpose VLMs with specialized gaze models under both zero-shot and fine-tuning settings. As a result, it remains unclear where modern VLMs stand on gaze understanding tasks, which tasks they can solve directly, and how much adaptation is needed to close the gap. This positioning is a necessary foundation for further applying VLMs to gaze understanding. Motivated by this gap, **EyeVLM** provides a unified evaluation of VLMs on gaze following and social gaze prediction across tasks, models, prompts, and adaptation settings.

### 3 EyeVLM Framework

We present **EyeVLM**, a unified evaluation framework for systematically investigating and benchmarking gaze understanding in VLMs, including comparisons with state-of-the-art vision-based models. In Section 3.1, we introduce the task formulations. Section 3.2 describes and motivates the prompting strategies we study, while Section 3.3 details our VLM fine-tuning approach.

#### 3.1 Task Formulation

We formulate both our tasks into a unified VLM-compatible visual question answering setting. Each sample consists of an image  $I$  and data  $B$  that specifies the subject(s) of interest. This information is used to generate a prompt  $Prompt$  that depends on the task and prompting strategy  $Q$ , and further passed through a VLM to generate a textual output  $J$  that included a structured JSON response, enabling automatic parsing to generate the result of interest  $O$  and evaluation. Formally, we have:

$$Prompt = Q^{Task, PromptStrategy}(I, B)$$
$$O = Parse^{Task}(J) \text{ with } J = VLM(Prompt)$$

**Gaze Following.** In that case, the input  $B$  simply consists of the subject head bounding box  $b = [x_{min}, y_{min}, x_{max}, y_{max}]$ , while the output is  $O = (p_{io}, (x, y))$ , which comprises the probability  $p_{io} \in [0, 1]$  that the gaze target lies inside the visible image area, and  $(x, y) \in [0, 1]^2$  denotes the normalized gaze point. Note that for Qwen models, we report  $(x, y) \in [0, 1000]^2$  as Qwen models are trained to use such scale for coordinates representation

**Social Gaze.** Here the input  $B$  comprises the two head bounding boxes  $b_1, b_2$  associated with the social relation that is being tested: LAEO, looking at each other, SA, shared attention between the two persons, LAH, is person  $b_1$  looking at person  $b_2$ 's face. In the three cases,  $O$  only comprises  $p_{sg} \in [0, 1]$ , which denotes the confidence that the queried social gaze behavior is true.

#### 3.2 Zero-shot Prompt Protocols

Many studies have shown that LLMs may perform better with different prompting strategies, especially in domains requiring logical reasoning such as mathematics and code generation [32, 33]. However, their use in VLMs has shown mixed results: while some works demonstrate improved accuracy [34, 35], others show that they can hurt performance, especially when perception is uncertain [36], as it can be in our case. As our goal is not only to measure zero-shot accuracy, but also to understand which aspects of the gaze tasks are already well captured by VLMs and which are not, we design four prompting strategies with progressively increasing levels of guidance. These strategies cover the two main prompting paradigms (Chain-of-Thought and in-context learning, also known as few-shot prompting), and allow us to systematically analyze prompt sensitivity and impact on performance measures. Below, we describe their main features, first focusing on gaze following, before detailing how they are adapted to social gaze tasks. Detailed prompts are in Appendix J and K.

**PRBASE.** This prompt comprises three components: a role description, a task description, and an input–output format description. The role description defines the model identity and provides the general semantic space for task-relevant behaviors:

"You are a vision assistant specializing in human gaze analysis."

The task description specifies the semantic goal of the queried task. For gaze following, this consists in asking where a person of interest is looking, including (i) the probability that the person's gaze target is within the frame, and (ii) the location of the gaze point within the scene. However, these two outputs are inherently coupled: if the model predicts that the person is looking outside the frame, it may trivially output a default gaze point (e.g.,  $[0, 0]$ ) rather than reasoning about the most probable gaze location. To address this coupling, we design the prompt to ensure that VLMs predict a plausible gaze point even when the person of interest is likely looking outside the frame. Finally, the format description explicitly constrains the expected JSON output.

**PRCOTBASE.** Chain-of-Thought (CoT) is a prompting strategy that encourages VLMs to perform step-by-step reasoning about a given task. While it is widely used to elicit intermediate reasoning, its benefits can extend beyond simple logical decomposition. In gaze understanding, effective prediction requires integrating multiple heterogeneous cues, including visual perception (e.g., head pose and eye direction), scene semantics (e.g., objects and interactions), and 3D spatial reasoning (e.g., relative positions and visibility). Such multi-factor reasoning is often implicit and not directly enforced by standard prompts. CoT provides a mechanism to externalize and structure this process, guiding

the model to sequentially attend to relevant cues and intermediate decisions. This is particularly important for VLMs, where reasoning must bridge visual and linguistic modalities. To evaluate whether VLMs can leverage such structured reasoning, we first consider a vanilla CoT prompt that augments the base prompt with an explicit instruction encouraging step-by-step analysis: To evaluate whether VLMs can leverage such structured reasoning, we first consider a vanilla CoT prompt that augments the base prompt with an explicit instruction encouraging step-by-step analysis:

"In order to achieve your task, you can first do a step-by-step analysis."

This variant allows us to assess whether explicitly eliciting intermediate reasoning improves performance on gaze understanding, and more importantly, whether VLMs can effectively ground this reasoning in visual evidence rather than relying on spurious or language-driven cues.

**PRCOTSTRUCT.** This prompt provides a more structured reasoning scaffold. Its motivation comes from the fact that while naive Chain-of-Thought prompting can be ineffective in VLMs, recent works suggest structured or guided variants significantly improve reasoning, particularly for spatial and visually grounded tasks [37–39] which share similarities with our task. We therefore guide the model through a sequence of intermediate questions, including: (1) describing the scene, (2) identifying the subject’s activity, (3) inferring gaze direction from head and eye cues, (4) enumerating plausible gaze targets inside the field of view, (5) describing spatial relations between the subject and candidate targets, and (6) synthesizing these cues into the final prediction. This prompt is intended to encourage models to attend to information that is particularly relevant for gaze reasoning.

**PRINCONTEXT-COT.** Studies have shown that directly providing examples to VLMs can be more effective than relying solely on explanation-only prompts, especially when these examples include CoT-guided reasoning [37]. To this end, this prompting strategy relies on two carefully selected in-context examples comprising an image, the question, the CoT process applied to that image, and the corresponding structured output. We manually write the analysis process for each example, considering all aspects mentioned in the PRCOTSTRUCT prompt. Samples are from the train sets. This variant tests whether exemplars help the model internalize both the expected reasoning pattern.

**Social Gaze Prompts.** They follow the same patterns as the gaze following ones. Only the task is adapted and defined as whether the queried pair of people exhibit a social gaze relation: looking-at-each-other (LAEO), shared attention (SA), or looking-at-person (LAH). Chain-of-Thought and In-Context prompts are adapted accordingly for each of the social task.

### 3.3 Supervised Fine-Tuning

While the previous section explores how far VLMs can be pushed through prompting alone, we now investigate whether supervised fine-tuning can further specialize VLMs for gaze understanding. Despite their strong general-purpose multimodal capabilities, VLMs are not explicitly trained to capture gaze and attention cues, which are critical for our tasks. We therefore study whether task-specific supervision can bridge this gap.

**QA Pair Construction.** Fine-tuning VLMs requires text-based QA pairs, while existing datasets for gaze following and social gaze prediction do not provide such annotations. To address this, we construct QA pairs for both gaze understanding tasks. As described in Section 3.1, each query specifies the task and localizes the person(s) of interest via subject head bounding box(es), combining a task-specific question template with the corresponding subject location. For gaze following, we further decompose the prediction into two separate queries: an `inout` query and a `gaze_point` query. We adopt this decoupled design because jointly predicting both outputs may introduce undesirable causal dependencies in the model responses, as discussed in Section 3.2. Querying these variables separately alleviates this issue and leads to more stable predictions. Accordingly, the task-specific question templates take the following form:

**Gaze Following and Social Gaze Prediction**

- *In/Out Query:* "Is the gaze target of <OnePerson> inside the frame?"
- *Gaze Point Query:* "Where is <OnePerson> looking at?"
- *LAEO:* "Are the <TwoPersons> in the image looking at each other?"
- *LAH:* "Is <OnePerson> looking at <OnePerson>?"
- *SA:* "Do <TwoPersons> appear to be sharing attention?"

<OnePerson>: the person whose head is within the bounding box  $[x_{\min}, y_{\min}, x_{\max}, y_{\max}]$

<TwoPersons>: the two individuals whose heads are enclosed by the bounding boxes  $[x_{\min}^{(1)}, y_{\min}^{(1)}, x_{\max}^{(1)}, y_{\max}^{(1)}]$  and  $[x_{\min}^{(2)}, y_{\min}^{(2)}, x_{\max}^{(2)}, y_{\max}^{(2)}]$

These are simple examples. To improve generalization, we design diverse question templates for each query type while preserving semantic consistency. In addition, we introduce varied linguistic expressions to specify subject location. During QA pair generation, these components are sampled independently and then combined to form the final queries, significantly increasing their diversity. Further details are provided in Appendix L. For the expected answers, we adopt a structured JSON format, as described in Section 3.2, to ensure consistency and facilitate learning.

**Adaptation Setup.** We adopt the standard LoRA-based supervised fine-tuning (rank 8, batch 64) using our constructed QA pairs, optimizing the standard next-token prediction objective. We resize images and constrain the total number of pixels to 200,704 ( $448 \times 448$ ) to align with other gaze works while preserving the aspect ratio of the images. More details in Appendix A.

## 4 Experiments

### 4.1 Experimental Protocol

We proposed an evaluation protocol enabling us to compare heterogeneous VLMs under a unified interface, despite differences in architecture, training data, and native output behavior. This includes comparisons with purely vision-based models.

**Datasets.** We rely on three datasets, **GazeFollow (GF)**, **VideoAttentionTarget (VAT)**, and **ChildPlay (CP)**, for training and evaluation. These datasets cover complementary settings, including static images, dynamic videos, and natural child–adult interactions, enabling a broad assessment of model performance on both gaze following and social gaze prediction tasks. See Appendix B for more details. In their original versions, these datasets provide annotations for gaze following, including head bounding boxes, gaze target locations, and in-frame versus out-of-frame labels (for VAT and ChildPlay). VSGaze [10] extends the annotations of several datasets [2, 21, 24, 8] to include social gaze behaviors. In this work, we use the extended annotations on VAT and ChildPlay to construct the social gaze prediction benchmark.

**Benchmarks.** For the gaze following task, we follow the standard train/test splits defined by each dataset. For the social gaze prediction task, the original data exhibit substantial class imbalance between positive and negative samples across the three categories, namely LAEO, LAH, and SA, as well as significant redundancy due to dense temporal annotations, which can bias training and evaluation. To address these issues, we re-sample the data and construct a balanced subset in which positive and negative samples are evenly distributed across all three categories. Both training and evaluation for social gaze prediction are conducted on this re-sampled dataset. Detailed sampling procedures and the resulting data distributions are provided in the supplementary material (Supp. C).

**Metrics.** For gaze following, we follow the standard evaluation protocol and report metrics commonly used in prior work: the average L2 distance between the predicted gaze point and the ground-truth target (with locations expressed in the  $[0, 1] \times [0, 1]$  normalized image space), and the average precision  $AP_{in/out}$  for in/out prediction. On the GazeFollow dataset, we additionally report the minimum distance between the predicted gaze point and multiple ground-truth targets. We further report the 2D angular error between the predicted and reference gaze directions, which measures how accurately the model infers head pose and gaze direction. For social gaze prediction, we report precision, recall, and F1 score for the three categories: LAH, LAEO, and SA.

**Output Parsing.** Since the model outputs JSON text, we first parse the response and extract the predicted variables for evaluation. In zero-shot evaluation, some models occasionally fail to follow the required output format. In this case, we map the output to predefined default values to ensure that all responses remain evaluable under a unified protocol. Concretely, we use a default value of 0.5 for `inout`, (0.5, 0.5) for `gaze_point`, and 0.5 for social gaze prediction. This fallback mechanism avoids discarding malformed generations and penalizes format non-compliance in a consistent way.

**Fine Tuning Approaches.** To follow recent gaze following work [10, 4], we first fine-tune the VLM on the gaze following task using the GF dataset, and then further fine-tune it on the target task and dataset (e.g., gaze following on VAT). We denote this approach by FTspec<sup>2</sup>. We also evaluate whether

<sup>2</sup>An exception is the MTGS model [10]. We use an updated version [40] that leverages a DINOv2 backbone, following [4]. This model is trained on the GF dataset and fine-tuned on VSGaze. We denote this as FTspec<sup>†</sup>.

Prompt	Gaze Following			Social Gaze Prediction		
	Avg L2 ↓	Min L2 ↓	Ang Err ↓	F1 <sub>LAH</sub> ↑	F1 <sub>LAE0</sub> ↑	F1 <sub>SA</sub> ↑
PRBASE	0.332	0.240	48.5°	<b>0.699</b>	<b>0.794</b>	<u>0.630</u>
PRCOTBASE	0.244	0.165	36.2°	0.691	0.749	0.608
PRCOTSTRUCT	<u>0.224</u>	<u>0.153</u>	<u>33.5°</u>	<u>0.695</u>	<u>0.768</u>	<b>0.633</b>
PRINCONTEXT-COT	<b>0.215</b>	<b>0.143</b>	<b>30.7°</b>	0.643	0.756	0.538

Table 1: **Comparison of prompting strategies for gaze following and social gaze prediction.** Results are obtained with *Qwen3-VL-8B-Instruct* [16], evaluated on GazeFollow [1] (GF) and VAT [2] (SG). CoT-based prompting significantly improves gaze following, while offering limited or inconsistent gains for social gaze prediction. Best in bold, second-best underlined.

(i) training with more data improves performance, denoted by AllD when using all three datasets (GF, VAT, CP) simultaneously; and (ii) joint training on multiple tasks improves results, as shown in prior work [10]. We denote these settings as GFo when training on the gaze following task only, and GFo+SG when adding social gaze supervision.

## 4.2 Zero-Shot Prompt Evaluation

We evaluate different prompting strategies on gaze following and social gaze prediction using the GazeFollow and VAT test sets, respectively, with *Qwen3-VL-8B-Instruct* [16] as a representative VLM. Results are reported in Table 1. Interestingly, we observe that prompting strategies exhibit markedly different behaviors across the two tasks.

For gaze following, CoT-based prompts (PRCOTBASE, PRCOTSTRUCT, PRINCONTEXT-COT) consistently outperform the non-CoT baseline PRBASE, indicating that the task requires structured reasoning to integrate multiple visual cues. Moreover, PRCOTSTRUCT further improves performance over PRCOTBASE by explicitly guiding the reasoning process. In particular, prompting the model to analyze head pose, gaze direction, and spatial relations between the subject and candidate targets leads to better localization accuracy and improved gaze direction prediction (lower angular errors). This corroborates prior work showing that structured or guided CoT is more effective than naive reasoning for visually grounded tasks [37, 39], and that CoT improves performance on tasks involving spatial reasoning and multi-step inference [34, 35]. Finally, augmenting this guidance with in-context examples (PRINCONTEXT-COT) provides additional gains, suggesting that exemplars help the model internalize both the reasoning process and the expected output format.

In contrast, for social gaze prediction, a simple prompt without CoT already achieves strong performance, while CoT-based variants bring limited or even negative gains. This suggests that the task relies more on high-level semantic understanding of the scene and of the situation than on precise geometric reasoning. In this context, by benefiting from large-scale language and vision-language pretraining, VLMs are already good at capturing the global context and relational cues required for social gaze prediction, making additional reasoning scaffolding less beneficial.

## 4.3 Gaze Following Evaluation

We evaluate three categories of methods: pure vision-based gaze models, zero-shot VLMs using the PRINCONTEXT-COT prompt, and fine-tuned VLMs with different training strategies. Results on GazeFollow and VAT are reported in Table 2, and results on ChildPlay (CP) in appendix (Table 6).

Specialized vision-based models remain the strongest for precise gaze target localization, while zero-shot VLMs lag behind by a large margin across all datasets. Although larger zero-shot models improve localization accuracy, the gains remain limited. Fine-tuning substantially reduces this gap: compared to zero-shot *Qwen3-VL-8B-Instruct*, its fine-tuned counterpart consistently lowers localization errors on GF, VAT, and CP. However, even after fine-tuning, VLMs still underperform the best specialized models in terms of L2 distance and angular error, particularly on VAT and CP. Joint training on all datasets (AllD) or adding social gaze supervision has limited impact overall (slightly worse on GF, similar on VAT, slightly better on CP). All this suggests that while VLMs contain transferable visual representations for gaze understanding, their architectures and training objectives remain suboptimal for fine-grained spatial prediction compared to dedicated gaze models. We also explore stochastic decoding by using a non-zero temperature. We observe that outputs tend to cluster around ambiguous candidate targets, and that averaging predictions consistently improves performance as the number of samples increases. More details are provided in Appendix E.

Table 4 further compares closed- and open-source VLMs. Gemini-3.1-Pro-Preview achieves the best performance, outperforming ChatGPT-5.4-Thinking and all open-source zero-shot models, indicating

Method	FT Strategy	GazeFollow			VideoAttentionTarget			
		Avg L2↓	Min L2↓	Ang Err↓	L2↓	Ang Err↓	AP <sub>in/out</sub> ↑	F1 <sub>in/out</sub> ↑
<i>One Human</i>	–	0.096	0.040	11.0°	0.051	–	0.925	–
Tonini [41]	FTspec	0.141	–	–	0.125	–	0.742	–
Hu [42]	FTspec	0.128	0.069	–	0.118	–	0.881	–
Gupta [19]	FTspec	0.114	0.056	–	0.110	–	0.879	–
Horanyi <sup>#</sup> [43]	FTspec	0.196	0.127	–	0.199	–	0.800	–
Miao [22]	FTspec	0.123	0.065	–	0.109	–	<b>0.908</b>	–
Tafasca [21]	FTspec	0.122	0.062	–	0.109	–	0.834	–
Tafasca [9]	FTspec	0.113	0.057	–	0.107	–	0.891	–
Gaze-LLE (ViT-B)* [4]	FTspec	0.104	0.045	12.4°	0.107	14.9°	0.898	0.841
Gaze-LLE (ViT-L)* [4]	FTspec	0.098	<b>0.041</b>	11.6°	0.103	13.3°	0.903	<b>0.875</b>
MTGS-DINO-static* [10]	FTspec <sup>‡</sup>	<b>0.094</b>	<b>0.041</b>	<b>11.0°</b>	<b>0.097</b>	<b>11.0°</b>	0.874	0.858
InternVL3.5-38B [44]	–	0.184	0.121	26.0°	0.250	38.4°	0.684	0.803
Qwen3-VL-32B-Instruct [16]	–	0.184	0.120	25.3°	0.229	32.8°	0.674	0.793
Qwen3-VL-8B-Instruct [16]	–	0.215	0.143	30.7°	0.249	38.5°	0.674	0.792
Qwen3-VL-8B-Instruct <sup>†</sup>	FTspec	0.110	0.049	14.5°	0.133	19.0°	0.787	0.809
Qwen3-VL-8B-Instruct <sup>†</sup>	AllD/GFo	0.112	0.052	14.4°	0.130	18.1°	0.786	0.812
Qwen3-VL-8B-Instruct <sup>†</sup>	AllD/GFo +SG	0.114	0.052	14.7°	0.132	19.7°	0.812	0.843

Table 2: Gaze following results on the GF and VAT datasets. We report results in three main blocks. Top: specialized vision-based gaze following methods (\*re-evaluated, #reimplementation version from Gaze-LLE). Middle: zero-shot VLM methods (with PRINCONTEXT-COT prompt). Bottom: fine-tuned VLMs, <sup>†</sup>with different training strategies (see Section 4.1.)

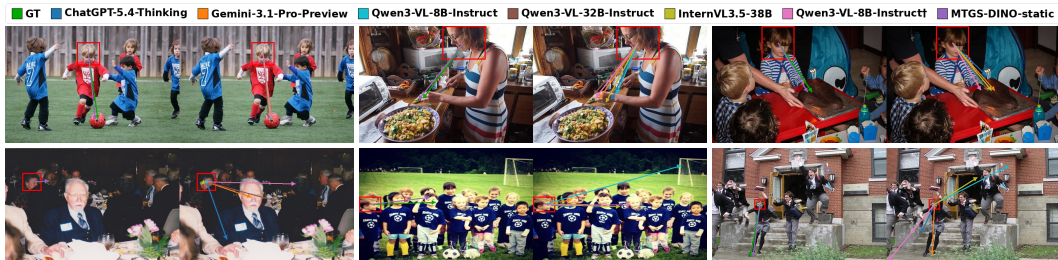


Figure 2: Qualitative results for gaze following on the GazeFollow dataset. For each sample, the left image shows the ground-truth (GT) and MTGS-DINO-static [40] predictions, while the right image presents predictions from different VLMs. Top: successful cases. Bottom: challenging scenarios (e.g., requiring depth understanding, involving multiple people, or targeting non-salient objects), where VLMs produce more diverse and less consistent predictions. Zoom in for better visualization.

that stronger closed-source VLMs exhibit better zero-shot gaze understanding.

Nevertheless, both remain behind the specialized MTGS-DINO-static model and the fine-tuned Qwen3-VL-8B-Instruct<sup>†</sup>. This confirms that, although closed-source VLMs provide stronger performance, task-specific fine-tuning remains necessary for accurate gaze target localization.

Fig. 2 displays predictions on sample images. They illustrate that while VLMs can predict accurate gaze points, they also struggle in more challenging cases and produce non-plausible results. We also conduct ablations on model size and training data scale in fine-tuning, see Appendix F and G.

#### 4.4 Social Gaze Prediction Evaluation

Table 3 reports social gaze results on VAT and ChildPlay for open-source VLMs compared to the specialized MTGS model, while Table 4 also includes closed-source models on a subset of VAT. Overall, we observe trends similar to gaze following: zero-shot open models lag behind MTGS, larger models perform better (Qwen 8B vs 32B), and closed-source models perform significantly better, with Gemini and ChatGPT achieving comparable results.

However, in contrast to gaze following, the performance gap with MTGS is much smaller. This trend is further confirmed after fine-tuning: VLMs not only improve substantially over their zero-shot counterparts and surpass closed-source models, but also reach performance close to the specialized model. While MTGS remains stronger on VAT, fine-tuned VLMs achieve better results on ChildPlay,

Method	FT Strategy	VAT [2]			ChildPlay [21]		
		F1 <sub>LAH</sub> ↑	F1 <sub>LAEO</sub> ↑	F1 <sub>SA</sub> ↑	F1 <sub>LAH</sub> ↑	F1 <sub>LAEO</sub> ↑	F1 <sub>SA</sub> ↑
MTGS-DINO-static [10]	FTspec ‡	<b>0.867</b>	<u>0.896</u>	<b>0.809</b>	0.740	0.873	<u>0.731</u>
InternVL3.5-38B [44]	–	0.698	0.767	0.655	0.703	0.789	0.620
Qwen3-VL-32B-Instruct [16]	–	0.696	0.826	0.689	0.662	0.791	0.574
Qwen3-VL-8B-Instruct [16]	–	0.699	0.794	0.630	0.648	0.769	0.520
Qwen3-VL-8B-Instruct†	FTspec	<u>0.829</u>	<b>0.929</b>	<u>0.714</u>	<u>0.789</u>	<u>0.887</u>	0.729
Qwen3-VL-8B-Instruct†	AllD/GFo+SG	0.808	0.894	0.707	<b>0.797</b>	<b>0.905</b>	<b>0.803</b>

Table 3: Social gaze prediction results on the VAT and ChildPlay datasets. Middle block: zero-shot VLM (with the PRBASE prompt). Bottom block: fine-tuned VLM (see Section 4.1). Best results are in bold, and second-best results are underlined.

Method	FT Strategy	Gaze Following			Social Gaze Prediction		
		Avg L2↓	Min L2↓	Ang Err↓	F1 <sub>LAH</sub> ↑	F1 <sub>LAEO</sub> ↑	F1 <sub>SA</sub> ↑
MTGS-DINO-static [10]	FTspec ‡	<b>0.096</b>	<b>0.043</b>	<b>11.0°</b>	<b>0.847</b>	<u>0.903</u>	<b>0.815</b>
ChatGPT-5.4-Thinking [45]	–	0.164	0.101	22.4°	0.769	0.879	0.717
Gemini-3.1-Pro-Preview [46]	–	0.131	0.069	16.4°	0.802	0.850	<u>0.726</u>
InternVL3.5-38B [44]	–	0.183	0.122	25.1°	0.694	0.767	0.655
Qwen3-VL-32B-Instruct [16]	–	0.175	0.113	24.3°	0.690	0.832	0.685
Qwen3-VL-8B-Instruct [16]	–	0.211	0.140	29.9°	0.706	0.804	0.628
Qwen3-VL-8B-Instruct†	FTspec	<u>0.107</u>	0.050	14.2°	<u>0.836</u>	<b>0.932</b>	0.723
Qwen3-VL-8B-Instruct†	AllD/GFo+SG	0.109	<u>0.049</u>	<u>13.5°</u>	0.802	0.883	0.716

Table 4: Comparison with closed-source VLMs. Gaze following is evaluated on the first 1K samples of the GF test set, social gaze prediction on a 1K-sample subset of the VAT test set (with 500 positive and 500 negative samples per task). Zero-shot VLMs use the PRINCONTEXT-COT prompt for gaze following, and PRBASE prompt for social gaze. Best results are in bold, second best are underlined.

particularly when trained on all datasets and combined with gaze-following supervision. Note however that the number of social gaze samples is lower on ChildPlay than on VAT (see Table 5 in appendix), which may slightly affect the results. In addition, the specific training setup of MTGS may also influence its performance on this dataset (see Appendix M). Nevertheless, the overall trend suggests that VLMs can approach the performance of specialized models on social gaze tasks.

A possible explanation, consistent with recent VLM literature [14], is that social gaze prediction relies more on high-level semantic and relational reasoning than on precise geometric localization. In particular, underlying LLMs encode rich knowledge about social concepts such as eye contact, shared attention, and human interactions, which enables a better understanding of the social situation depicted in the scene. Through vision-language alignment, VLMs can leverage this knowledge to interpret interactions and intentions, which may explain why, despite weaker gaze-following performance, they achieve comparable results on social gaze tasks. Further work is needed to validate this hypothesis by more explicitly analyzing their reasoning processes.

## 5 Conclusion

We presented a systematic study of gaze understanding in vision-language models by evaluating gaze following and social gaze prediction under a unified VQA formulation. Experiments on GazeFollow, VAT, and ChildPlay show that zero-shot VLMs remain limited in precise gaze reasoning, while task-specific fine-tuning substantially improves performance across datasets and tasks. Notably, fine-tuned VLMs achieve competitive performance on social gaze prediction, approaching specialized state-of-the-art models, suggesting that VLMs can effectively capture high-level human gaze relations after supervision. However, their performance on gaze following remains clearly behind dedicated gaze models, highlighting persistent limitations in precise spatial grounding and subject-conditioned localization. Overall, these results indicate that generic vision-language pretraining alone is insufficient for reliable gaze target estimation, and that gaze understanding remains a challenging capability for current VLMs. We hope that EyeVLM will serve as a foundation for better understanding these limitations and for developing future gaze-aware VLMs.

## References

- [1] A. Recasens, A. Khosla, C. Vondrick, and A. Torralba, “Where are they looking?” in *Advances in Neural Information Processing Systems (NeurIPS)*, 2015. [Online]. Available: <https://papers.neurips.cc/paper/5848-where-are-they-looking.pdf>
- [2] E. Chong, Y. Wang, N. Ruiz, and J. M. Rehg, “Detecting attended visual targets in video,” in *Proceedings of the IEEE/CVF Conference on Computer Vision and Pattern Recognition (CVPR)*, 2020, pp. 5396–5406. [Online]. Available: [https://openaccess.thecvf.com/content\\_CVPR\\_2020/papers/Chong\\_Detecting\\_Attended\\_Visual\\_Targets\\_in\\_Video\\_CVPR\\_2020\\_paper.pdf](https://openaccess.thecvf.com/content_CVPR_2020/papers/Chong_Detecting_Attended_Visual_Targets_in_Video_CVPR_2020_paper.pdf)
- [3] N. J. Emery, “The eyes have it: The neuroethology, function and evolution of social gaze,” *Neuroscience & Biobehavioral Reviews*, vol. 24, no. 6, pp. 581–604, 2000.
- [4] F. Ryan, A. Bati, S. Lee, D. Bolya, J. Hoffman, and J. M. Rehg, “Gaze-ll: Gaze target estimation via large-scale learned encoders,” in *Proceedings of the IEEE/CVF Conference on Computer Vision and Pattern Recognition (CVPR)*, 2025. [Online]. Available: [https://openaccess.thecvf.com/content/CVPR2025/papers/Ryan\\_Gaze-LLE\\_Gaze\\_Target\\_Estimation\\_via\\_Large-Scale\\_Learned\\_Encoders\\_CVPR\\_2025\\_paper.pdf](https://openaccess.thecvf.com/content/CVPR2025/papers/Ryan_Gaze-LLE_Gaze_Target_Estimation_via_Large-Scale_Learned_Encoders_CVPR_2025_paper.pdf)
- [5] A. Frischen, A. P. Bayliss, and S. P. Tipper, “Gaze cueing of attention: Visual attention, social cognition, and individual differences,” *Psychological Bulletin*, vol. 133, no. 4, pp. 694–724, 2007.
- [6] M. J. Marin-Jimenez, V. Kalogeiton, P. Medina-Suarez, and A. Zisserman, “Laeo-net++: Revisiting people looking at each other in videos,” *arXiv preprint arXiv:2101.02136*, 2021. [Online]. Available: <https://arxiv.org/abs/2101.02136>
- [7] A. Gupta, S. Tafasca, N. Chutisilp, and J.-M. Odobez, “A unified model for gaze following and social gaze prediction,” in *IEEE International Conference on Automatic Face and Gesture Recognition (FG)*, 2024. [Online]. Available: [https://publications.idiap.ch/attachments/papers/2024/Gupta\\_FG\\_2024.pdf](https://publications.idiap.ch/attachments/papers/2024/Gupta_FG_2024.pdf)
- [8] L. Fan, W. Chen, P. Wei, S.-K. Yeung, T. Wong, and J. Xing, “Inferring shared attention in social scene videos,” in *Proceedings of the IEEE Conference on Computer Vision and Pattern Recognition (CVPR)*, 2018. [Online]. Available: [https://openaccess.thecvf.com/content\\_cvpr\\_2018/papers/Fan\\_Inferring\\_Shared\\_Attention\\_CVPR\\_2018\\_paper.pdf](https://openaccess.thecvf.com/content_cvpr_2018/papers/Fan_Inferring_Shared_Attention_CVPR_2018_paper.pdf)
- [9] S. Tafasca, A. Gupta, and J.-M. Odobez, “Sharingan: A transformer architecture for multi-person gaze following,” in *Proceedings of the IEEE/CVF Conference on Computer Vision and Pattern Recognition (CVPR)*, 2024. [Online]. Available: [https://openaccess.thecvf.com/content/CVPR2024/papers/Tafasca\\_Sharingan\\_A\\_Transformer\\_Architecture\\_for\\_Multi-Person\\_Gaze\\_Following\\_CVPR\\_2024\\_paper.pdf](https://openaccess.thecvf.com/content/CVPR2024/papers/Tafasca_Sharingan_A_Transformer_Architecture_for_Multi-Person_Gaze_Following_CVPR_2024_paper.pdf)
- [10] A. Gupta, S. Tafasca, A. Farkhondeh, P. Vuillecard, and J.-M. Odobez, “Mtgs: A novel framework for multi-person temporal gaze following and social gaze prediction,” in *Advances in Neural Information Processing Systems (NeurIPS)*, 2024. [Online]. Available: <https://arxiv.org/abs/2403.10511>
- [11] A. Radford, J. W. Kim, C. Hallacy, A. Ramesh, G. Goh, S. Agarwal, G. Sastry, A. Askell, P. Mishkin, J. Clark, G. Krueger, and I. Sutskever, “Learning transferable visual models from natural language supervision,” in *Proceedings of the International Conference on Machine Learning (ICML)*, 2021. [Online]. Available: <https://arxiv.org/abs/2103.00020>
- [12] J. Li, D. Li, S. Savarese, and S. Hoi, “Blip-2: Bootstrapping language-image pre-training with frozen image encoders and large language models,” in *Proceedings of the International Conference on Machine Learning (ICML)*, 2023. [Online]. Available: <https://arxiv.org/abs/2301.12597>
- [13] H. Liu, C. Li, Q. Wu, and Y. J. Lee, “Visual instruction tuning,” in *Advances in Neural Information Processing Systems (NeurIPS)*, 2023. [Online]. Available: <https://arxiv.org/abs/2304.08485>
- [14] S. Huang, L. Dong, W. Wang, Y. Yang, F. Wang, F. Liu, Z. Chi, T. Zhang, Q. Li, F. Lin *et al.*, “Kosmos-1: Multimodal large language model in the wild,” *arXiv preprint arXiv:2302.14045*, 2023.
- [15] B. Thumu, L. Mathur, Y. Kebe, and L.-P. Morency, “Social caption: Evaluating social understanding in multimodal models,” 2026. [Online]. Available: <https://arxiv.org/abs/2601.14569>
- [16] Q. Team, “Qwen3 technical report,” 2025. [Online]. Available: <https://arxiv.org/abs/2505.09388>
- [17] Y. Fang, J. Tang, W. Shen, W. Shen, X. Gu, L. Song, and G. Zhai, “Dual attention guided gaze target detection in the wild,” in *Proceedings of the IEEE/CVF conference on computer vision and pattern recognition*, 2021, pp. 11 390–11 399.

- [18] D. Lian, Z. Yu, and S. Gao, “Believe it or not, we know what you are looking at!” in *Asian Conference on Computer Vision*. Springer, 2018, pp. 35–50.
- [19] A. Gupta, S. Tafasca, and J.-M. Odobez, “A modular multimodal architecture for gaze target prediction: Application to privacy-sensitive settings,” in *Proceedings of the IEEE/CVF Conference on Computer Vision and Pattern Recognition Workshops (CVPRW)*, 2022, pp. 5041–5050.
- [20] T. Jin, Q. Yu, S. Zhu, Z. Lin, J. Ren, Y. Zhou, and W. Song, “Depth-aware gaze-following via auxiliary networks for robotics,” *Engineering Applications of Artificial Intelligence*, vol. 113, p. 104924, 2022.
- [21] S. Tafasca, A. Gupta, and J.-M. Odobez, “Childplay: A new benchmark for understanding children’s gaze behaviour,” in *Proceedings of the IEEE/CVF international conference on computer vision*, 2023, pp. 20935–20946.
- [22] Q. Miao, M. Hoai, and D. Samaras, “Patch-level gaze distribution prediction for gaze following,” in *Proceedings of the IEEE/CVF Winter Conference on Applications of Computer Vision (WACV)*, 2023, pp. 880–889. [Online]. Available: [https://openaccess.thecvf.com/content/WACV2023/papers/Miao\\_Patch-Level\\_Gaze\\_Distribution\\_Prediction\\_for\\_Gaze\\_Following\\_WACV\\_2023\\_paper.pdf](https://openaccess.thecvf.com/content/WACV2023/papers/Miao_Patch-Level_Gaze_Distribution_Prediction_for_Gaze_Following_WACV_2023_paper.pdf)
- [23] M. J. Marin-Jimenez, A. Zisserman, M. Eichner, and V. Ferrari, “Detecting people looking at each other in videos,” *International Journal of Computer Vision (IJCV)*, 2013. [Online]. Available: <https://www.robots.ox.ac.uk/~vgg/publications/2014/Marin14/marin14.pdf>
- [24] M. J. Marin-Jimenez, V. Kalogeiton, P. Medina-Suarez, and A. Zisserman, “Laeo-net: Revisiting people looking at each other in videos,” in *Proceedings of the IEEE/CVF Conference on Computer Vision and Pattern Recognition (CVPR)*, 2019. [Online]. Available: [https://openaccess.thecvf.com/content\\_CVPR\\_2019/papers/Marin-Jimenez\\_LAEO-Net\\_Revisiting\\_People\\_Looking\\_at\\_Each\\_Other\\_in\\_Videos\\_CVPR\\_2019\\_paper.pdf](https://openaccess.thecvf.com/content_CVPR_2019/papers/Marin-Jimenez_LAEO-Net_Revisiting_People_Looking_at_Each_Other_in_Videos_CVPR_2019_paper.pdf)
- [25] B. Doosti, C.-H. Chen, R. Vemulapalli, X. Jia, Y. Zhu, and B. Green, “Boosting image-based mutual gaze detection using pseudo 3d gaze,” *Proceedings of the AAAI Conference on Artificial Intelligence*, vol. 35, no. 2, pp. 1273–1281, May 2021. [Online]. Available: <https://ojs.aaai.org/index.php/AAAI/article/view/16215>
- [26] G. Cantarini, F. F. Tomenotti, N. Noceti, and F. Odone, “Hhp-net: A light heteroscedastic neural network for head pose estimation with uncertainty,” 2021.
- [27] Ö. Sümer, P. Gerjets, U. Trautwein, and E. Kasneci, “Attention flow: End-to-end joint attention estimation,” in *Proceedings of the IEEE/CVF Winter Conference on Applications of Computer Vision (WACV)*, 2020. [Online]. Available: [https://openaccess.thecvf.com/content\\_WACV\\_2020/papers/Sumer\\_Attention\\_Flow\\_End-to-End\\_Joint\\_Attention\\_Estimation\\_WACV\\_2020\\_paper.pdf](https://openaccess.thecvf.com/content_WACV_2020/papers/Sumer_Attention_Flow_End-to-End_Joint_Attention_Estimation_WACV_2020_paper.pdf)
- [28] A. Gupta, P. Vuillecard, A. Farkhondeh, and J.-M. Odobez, “Exploring the zero-shot capabilities of vision-language models for improving gaze following,” in *Proceedings of the IEEE/CVF conference on computer vision and pattern recognition*, 2024, pp. 615–624.
- [29] Y. Yang and F. Lu, “Gazellm: a plug-and-play zero-shot llm reasoning framework for boosting gaze target detection,” *Visual Intelligence*, vol. 3, no. 1, p. 26, 2025.
- [30] A. M. Mathew, H. Hermassi, T. Khalid, and A. A. Khan, “GazeVlm: A vision-language model for multi-task gaze understanding,” *arXiv preprint arXiv:2511.06348*, 2025.
- [31] S. Wang, C. Cui, Y. Huang, H. J. Chang, and Y. Cheng, “Vl4gaze: Unleashing vision-language models for gaze following,” *arXiv preprint arXiv:2512.20735*, 2025.
- [32] J. Wei, X. Wang, D. Schuurmans, M. Bosma, B. Ichter, F. Xia, E. H. Chi, Q. V. Le, and D. Zhou, “Chain-of-thought prompting elicits reasoning in large language models,” in *Advances in Neural Information Processing Systems (NeurIPS)*, 2022.
- [33] T. Kojima, S. Gu, M. Reid, Y. Matsuo, and Y. Iwasawa, “Large language models are zero-shot reasoners,” *arXiv preprint arXiv:2205.11916*, 2022.
- [34] P. Lu, S. Mishra, T. Xia, L. Qiu, K.-W. Chang, S.-C. Zhu, O. Tafjord, P. Clark, and A. Kalyan, “Learn to explain: Multimodal reasoning via thought chains for science question answering,” in *Advances in Neural Information Processing Systems (NeurIPS)*, 2022.
- [35] Z. Zhang, A. Zhang, M. Li, H. Zhao, G. Karypis, and A. Smola, “Multimodal chain-of-thought reasoning in language models,” *Transactions on Machine Learning Research (TMLR)*, 2024.

- [36] Y. Wu, Z. Yang, J. Qian, S. Gao, G. Chen, Q. Li, Y.-A. Huang, and Z.-A. Huang, “Better eyes, better thoughts: Why vision chain-of-thought fails in medicine,” *arXiv preprint arXiv:2603.06665*, 2026.
- [37] Z.-F. Chen *et al.*, “Visual chain-of-thought prompting for knowledge-based visual reasoning,” in *Proceedings of the AAAI Conference on Artificial Intelligence*, 2024.
- [38] J. Ge, H. Luo, S. Qian, Y. Gan, J. Fu, and S. Zhang, “Chain of thought prompt tuning in vision language models,” *arXiv preprint arXiv:2304.07919*, 2023.
- [39] B. Ji, S. Agrawal, Q. Tang, and Y. Wu, “Enhancing spatial reasoning in vision-language models via chain-of-thought prompting and reinforcement learning,” *arXiv preprint arXiv:2507.13362*, 2025.
- [40] A. Gupta, “mtgs-static-vsgaze,” 2026, accessed: 2026-05-06. [Online]. Available: <https://huggingface.co/ldiap/mtgs-static-vsgaze>
- [41] F. Tonini, C. Beyan, and E. Ricci, “Multimodal across domains gaze target detection,” in *Proceedings of the 2022 International Conference on Multimodal Interaction*, 2022, pp. 420–431.
- [42] Z. Hu, K. Zhao, B. Zhou, H. Guo, S. Wu, Y. Yang, and J. Liu, “Gaze target estimation inspired by interactive attention,” *IEEE Transactions on Circuits and Systems for Video Technology*, vol. 32, no. 12, pp. 8524–8536, 2022.
- [43] N. Horanyi, L. Zheng, E. Chong, A. Leonardis, and H. J. Chang, “Where are they looking in the 3d space?” in *Proceedings of the IEEE/CVF Conference on Computer Vision and Pattern Recognition Workshops (CVPRW)*, 2023, pp. 2678–2687.
- [44] W. Wang, Z. Gao, L. Gu, H. Pu, L. Cui, X. Wei, Z. Liu, L. Jing, S. Ye, J. Shao *et al.*, “InternV3.5: Advancing open-source multimodal models in versatility, reasoning, and efficiency,” *arXiv preprint arXiv:2508.18265*, 2025.
- [45] OpenAI, “Gpt-5.4 thinking system card,” <https://openai.com/index/gpt-5-4-thinking-system-card/>, 2026.
- [46] Google DeepMind, “Gemini 3.1 pro model card,” <https://deepmind.google/models/model-cards/gemini-3-1-pro/>, 2026.
- [47] Y. Zheng, R. Zhang, J. Zhang, Y. Ye, Z. Luo, Z. Feng, and Y. Ma, “Llamafactory: Unified efficient fine-tuning of 100+ language models,” in *Proceedings of the 62nd Annual Meeting of the Association for Computational Linguistics (Volume 3: System Demonstrations)*. Bangkok, Thailand: Association for Computational Linguistics, 2024. [Online]. Available: <http://arxiv.org/abs/2403.13372>
- [48] W. Kwon, Z. Li, S. Zhuang, Y. Sheng, L. Zheng, C. H. Yu, J. E. Gonzalez, H. Zhang, and I. Stoica, “Efficient memory management for large language model serving with pagedattention,” in *Proceedings of the ACM SIGOPS 29th Symposium on Operating Systems Principles*, 2023.
- [49] C. Lord, M. Rutter, S. Goode, J. Heemsbergen, H. Jordan, L. Mawhood, and E. Schopler, “Autism diagnostic observation schedule: A standardized observation of communicative and social behavior,” *Journal of autism and developmental disorders*, vol. 19, no. 2, pp. 185–212, 1989.
- [50] Lord, Rutter, DiLavore, Risi, Gotham, and Bishop, “Autism Diagnostic Observation Schedule, Second Edition,” 2012.

## A Implementation Details

We fine-tune representative Qwen-based VLMs on the constructed QA pairs using LLaMA-Factory [47]. Specifically, LoRA adapters are inserted into both the self-attention projection layers (`q_proj`, `k_proj`, `v_proj`, and `o_proj`) and the gated feed-forward projection layers (`gate_proj`, `up_proj`, and `down_proj`). The vision encoder and language modeling head are kept frozen. We set the LoRA rank to 8, the batch size to 64, and the learning rate to  $4.0 \times 10^{-4}$ .

Although Qwen3-VL models can be trained with native-resolution images, we resize all images while preserving their aspect ratios and constrain the total number of pixels to 200,704 ( $448 \times 448$ ), following the resolution commonly used in prior gaze works. The model is trained with the standard next-token prediction objective on the target JSON text. Under this setup, gaze understanding is learned through the conventional language modeling loss over structured textual outputs.

Training is conducted on a single NVIDIA H100 GPU for 2 epochs for the gaze following task. For social gaze prediction, we observe overfitting during training and therefore select checkpoints based on the validation sets of VAT and ChildPlay. For fine-tuning with FTspec, we report the results at 500 training steps. For fine-tuning with AllD/GFo+SG, we report the results at 5,000 training steps. To improve model generalization, we randomly sample a question for each training instance at every epoch. During inference, we uniformly use the vLLM [48] framework and disable sampling for deterministic and reproducible predictions.

## B Datasets

We use three datasets, **GazeFollow**, **VideoAttentionTarget (VAT)**, and **ChildPlay**, for training and evaluation. These datasets cover complementary settings, as presented below.

**GazeFollow [1]** is a large-scale benchmark for gaze following in natural images. It is collected from multiple public image sources, including SUN, MS COCO, ImageNet, and Places, and contains diverse daily scenes and activities. The dataset includes 122,143 images and 130,339 annotated person instances. Its annotations provide head location information together with the corresponding 2D gaze target, making it a standard benchmark for learning gaze target localization from head cues and scene context.

**VideoAttentionTarget (VAT) [2]** extends gaze following from static images to videos and emphasizes temporal modeling in dynamic scenes. It is constructed from 50 YouTube shows and contains 1,331 video clips, 71,666 frames, and 164,541 frame-level annotations. For each subject, VAT provides dense head bounding boxes and gaze point annotations, and also distinguishes whether the gaze target is inside or outside the image frame. Compared with GazeFollow, VAT contains less image diversity but is more suitable for evaluating temporal reasoning (whenever a temporal model is used) and in-frame versus out-of-frame gaze prediction.

**ChildPlay [21]** is a benchmark designed for understanding gaze behavior in natural child-centered interactions. It contains 401 short videos collected from multiple online sources, comprising 120,549 frames and about 257,928 annotated instances. In addition to head bounding boxes and 2D gaze points, ChildPlay provides fine-grained gaze labels and child/adult identity annotations. Compared with conventional datasets that mainly focus on adults, ChildPlay presents more challenging interaction patterns and greater behavioral diversity, making it particularly valuable for evaluating gaze understanding in child-adult social scenarios.

## C Social Gaze Dataset Sampling

We sample social gaze labels from VSGaze [10], focusing on the ChildPlay [21] and VideoAttentionTarget [2] datasets because they provide high-resolution images and cover a diverse range of social interaction scenarios, from TV interviews to child-caregiver interactions. First, to reduce temporal redundancy, we only retain every third frame. Second, for each task, we sample negative social gaze relation pairs to match the number of positive pairs, yielding a balanced set of examples. We further discard small head bounding boxes, as well as social gaze annotations that occur near the boundaries of gaze events, such as shared attention. These boundary cases can be ambiguous because participants may be in the middle of a gaze shift. The resulting dataset statistics for each task and dataset are summarized in Table 5. Because VSGaze represents directed pairs, a pair of people may

Task	VAT		ChildPlay	
	Ordered (Pos/Neg)	Unordered (Pos/Neg)	Ordered (Pos/Neg)	Unordered (Pos/Neg)
LAH	4736/4736	-	2198/2198	-
LAEO	1874/1874	937/1825	426/426	213/425
SA	1958/1958	979/1768	538/538	269/503

Table 5: Number of positive and negative pairs for the social gaze tasks across VAT and ChildPlay.

Method	FT Strategy	L2↓	Ang Err↓	AP <sub>in/out</sub> ↑	F1 <sub>in/out</sub> ↑
Gupta [19]	FTspec	0.113	-	0.983	-
Tafasca [21]	FTspec	0.107	-	0.986	-
Tafasca [9]	FTspec	0.106	-	0.990	-
Gaze-LLE (ViT-B) [4]	FTspec	0.106	-	<b>0.994</b>	-
Gaze-LLE (ViT-L) [4]	FTspec	0.101	-	<b>0.994</b>	-
MTGS-DINO-static* [10]	FTspec <sup>‡</sup>	<b>0.099</b>	<b>9.4°</b>	<b>0.994</b>	0.972
InternVL3.5-38B [44]	-	0.212	29.9°	0.944	0.970
Qwen3-VL-32B-Instruct [16]	-	0.171	21.9°	0.946	0.969
Qwen3-VL-8B-Instruct [16]	-	0.245	32.2°	0.946	0.968
Qwen3-VL-8B-Instruct <sup>†</sup>	FTspec	0.122	12.7°	0.961	0.974
Qwen3-VL-8B-Instruct <sup>†</sup>	AllD/GFo	0.118	13.1°	0.966	0.972
Qwen3-VL-8B-Instruct <sup>†</sup>	AllD/GFo+SG	0.116	12.5°	0.969	0.969

Table 6: Gaze following results on ChildPlay. (\*Re-evaluated. †Fine-tuned.)

appear as both  $(A, B)$  and  $(B, A)$ . Therefore, we also report the number of unique unordered pairs in the table for LAEO and SA.

## D Additional Gaze Following Results

### D.1 Gaze Following Results on ChildPlay

Table 6 compares gaze following performance on ChildPlay. Zero-shot VLMs show competitive in/out prediction ability, achieving AP<sub>in/out</sub> and F1<sub>in/out</sub> scores close to specialized models, but their localization accuracy remains clearly worse, as indicated by larger L2 and angular errors. Fine-tuning substantially improves VLM localization performance, reducing the L2 error of Qwen3-VL-8B-Instruct from 0.245 to 0.122 and the angular error from 32.2° to 12.7°. Further using full gaze-following data and joint training with social gaze prediction brings additional gains, with *Full-GF+SG* achieving the best VLM localization result. Nevertheless, a gap remains between fine-tuned VLMs and specialized gaze models, suggesting that VLMs are strong at in/out prediction but still less accurate in precise gaze target localization.

### D.2 Cross-Dataset Evaluation

Table 7 shows the cross-dataset performance of Qwen3-VL-8B-Instruct when fine-tuned only on GazeFollow and directly evaluated on VAT and ChildPlay. The model achieves reasonable L2 errors of 0.130 and 0.119, respectively. This suggests that GazeFollow fine-tuning enables VLMs to learn gaze localization cues that can transfer to unseen datasets. Nevertheless, a noticeable gap remains compared with most of specialized models, indicating that current VLMs still require stronger domain adaptation or task-specific training for robust cross-dataset gaze target localization.

## E Effect of Sampling Strategy

We compare Best-of- $N$  and Average-of- $N$  aggregation strategies under different numbers of samples, with the results shown in Table 8. The results show that stochastic sampling can generate better gaze predictions when multiple candidates are considered. While a single sampled output with Temp. = 0.7 is worse than deterministic decoding, Best-of- $N$  consistently improves with larger  $N$ ,

Method	VAT	ChildPlay
	L2↓	L2↓
Chong [2]*	0.119	0.121
Jin [20]	0.104	–
Miao [22]*	0.109	0.113
Gupta [19]	0.137	0.142
Tafasca [21]	0.123	0.115
Gaze-LLE (B) [4]	0.105	0.114
Gaze-LLE (L) [4]	<b>0.100</b>	<b>0.101</b>
Qwen3-VL-8B-Instruct <sup>†</sup>	0.130	0.119

Table 7: Cross-dataset results on VAT [2] and ChildPlay [21]. The model is only fine-tuned on GazeFollow [1] dataset. \*: results evaluated by us based on official code releases.

$N$	Temp.	Best-of- $N$			Average-of- $N$		
		Avg L2↓	Min L2↓	Ang Err↓	Avg L2↓	Min L2↓	Ang Err↓
1	0.0	0.110	0.049	14.5°	0.110	0.049	14.5°
1	0.7	0.116	0.057	15.1°	0.116	0.057	15.1°
2	0.7	0.092	0.044	12.0°	0.106	0.054	13.8°
4	0.7	0.073	0.034	9.2°	0.099	0.051	13.0°
8	0.7	0.062	0.031	7.8°	0.097	0.051	12.7°
16	0.7	<b>0.055</b>	<b>0.030</b>	<b>6.9°</b>	<b>0.096</b>	<b>0.051</b>	<b>12.6°</b>

Table 8: Comparison of Best-of- $N$  and Average-of- $N$  aggregation strategies on GazeFollow.  $N$  denotes the number of samples, and Temp. denotes the sampling temperature. Best-of- $N$  selects the best sampled prediction, while Average-of- $N$  averages all sampled predictions.

reducing Avg L2 from 0.116 at  $N = 1$  to 0.055 at  $N = 16$ . This indicates that diverse samples often contain highly accurate candidates. However, Best-of- $N$  relies on selecting the best prediction among sampled outputs and therefore reflects an upper-bound setting. In comparison, Average-of- $N$  yields only modest improvements, suggesting that averaging improves prediction stability but cannot fully exploit the best individual samples.

## F Ablation of Model Size in Fine-tuning

Table 9 studies the effect of model size under the same fine-tuning setting. On GazeFollow [1], increasing the model size generally improves gaze localization, with Qwen3-VL-8B-Instruct<sup>†</sup> achieving the best Avg L2, Min L2, and angular error. However, this trend does not consistently transfer to cross-dataset evaluation on VAT [2] and ChildPlay [21]. Qwen3-VL-4B-Instruct<sup>†</sup> obtains the best or tied-best performance on both datasets, slightly outperforming the 8B model in L2 distance and angular error. These results suggest that larger VLMs can better fit the in-domain gaze-following task, but model scaling alone does not necessarily lead to better cross-dataset generalization.

## G Ablation of Training Data Scale in Fine-tuning

Table 10 shows the impact of GazeFollow training data scale on Qwen3-VL-8B-Instruct. Performance improves consistently as the amount of fine-tuning data increases, with Avg L2 decreasing from 0.191 at 1k samples to 0.120 at 50k samples, and angular error dropping from 25.4° to 16.0°. Using the full training set further improves all metrics, achieving the best Avg L2 of 0.110 and angular error of 14.5°. This demonstrates that gaze following benefits substantially from larger-scale task-specific supervision, although performance gains become more gradual at larger data scales.

Method	GazeFollow [1]			VAT [2]		ChildPlay [21]	
	Avg L2↓	Min L2↓	Ang Err↓	L2↓	Ang Err↓	L2↓	Ang Err↓
Qwen3-VL-2B-Instruct <sup>†</sup>	0.121	0.059	16.1°	0.131	19.5°	0.122	14.1°
Qwen3-VL-4B-Instruct <sup>†</sup>	0.113	0.051	14.8°	<b>0.126</b>	<b>18.2°</b>	<b>0.117</b>	<b>13.1°</b>
Qwen3-VL-8B-Instruct <sup>†</sup>	<b>0.110</b>	<b>0.049</b>	<b>14.5°</b>	0.130	18.3°	0.119	<b>13.1°</b>

Table 9: Ablation on model size for fine-tuning. VAT and ChildPlay evaluations are cross dataset evaluation.

Data Scale	Avg L2↓	Min L2↓	Ang Err↓
1k	0.191	0.120	25.4°
3k	0.177	0.109	23.9°
5k	0.155	0.088	21.8°
10k	0.142	0.077	20.5°
50k	0.120	0.058	16.0°
Full	<b>0.110</b>	<b>0.049</b>	<b>14.5°</b>

Table 10: GazeFollow test results of Qwen3-VL-8B-Instruct under different GazeFollow training sizes, compared with the mainline full-data model. Lower is better for all metrics.

## H Ablation of PRINCONTEXT-COT Prompt Settings

Table 11 compares different in-context example settings on GazeFollow. Image-text demonstrations outperform text-only demonstrations, and using two image-text examples achieves the best results across all metrics. This indicates that visual demonstrations provide helpful task cues for gaze localization.

## I Head Localization Sensitivity Evaluation

One of the key assumptions in this work is that VLMs are capable of understanding head localization inputs. In this section, we verify this assumption by benchmarking the ability of VLMs to identify a person’s head given a bounding box as input. The objective is to construct a balanced dataset of positive bounding boxes containing a person’s head and negative bounding boxes containing none, then evaluate prompting strategies for head presence detection.

**Dataset.** We manually selected a subset of 189 images from the VAT test set, drawn from different videos and excluding images in which heads are unannotated (e.g., small heads in the background). For each annotated head in each image, a corresponding negative bounding box is generated with no overlap with any ground-truth head. Figure 3a illustrates both sets: ground-truth positive boxes are shown in green and generated negative boxes in blue. The resulting dataset comprises 958 question-answering pairs, balanced with 50% positive and 50% negative examples.

**Settings.** We evaluate the *Qwen3-VL-8B-Instruct* model on this task. All images are resized so that the longest side is 448 pixels while preserving the original aspect ratio. We compare two bounding box input representations: coordinates normalized to the range  $[0, 1000]$  and coordinates normalized to the range  $[0, 1]$ . In both cases, the model is queried with the following prompt:

Look at the region defined by the bounding box coordinate <bounding box coordinates>. Is there a person's head inside this bounding box? Answer only `Yes` or `No`.

**Results.** We report both accuracy and sensitivity; the latter is the primary metric of interest, since all experiments in the main paper use only positive head bounding boxes as input.

As shown in Table 12, the model achieves a sensitivity of 0.94, demonstrating a strong ability to recognize the presence of a head when a positive bounding box is provided. However, accuracy drops to 0.88, revealing a tendency to predict “yes” even for negative boxes. This suggests that the

Modality	# Examples	Avg L2↓	Min L2↓	Ang Err↓
T	2	0.193	0.127	27.3°
I+T	1	0.189	0.125	26.2°
I+T	2	<b>0.184</b>	<b>0.120</b>	<b>25.3°</b>

Table 11: Ablation study on in-context example settings for Qwen3-VL-32B-Instruct on GazeFollow. T denotes text-only examples, while I+T denotes image-text examples.

Setting	Accuracy↑	Sensitivity↑
Normalized 0–1	0.77	0.94
Normalized 0–1000	0.88	0.94

Table 12: Ablation localization results under different input normalization coordinates.

model does not precisely localize bounding box coordinates, but rather makes predictions based on approximate spatial reasoning. This is further supported by the distance analysis in Figure 3b, which shows that false positives on negative boxes tend to occur when those boxes are in close proximity to a ground-truth head.

Overall, these results confirm that Qwen3 can approximately localize bounding box coordinates and reliably identify a person’s head when a positive bounding box is provided as input, validating the core assumption of our approach.

## J Zero-Shot Prompts for GFo

For simplicity, we use `<Task description>` to denote the following description of the gaze following task.

```
You are a vision assistant specializing in human gaze analysis. Your task is to analyze an input image and determine where a person of interest is looking at. You must output two things:
```

- **inout**: a float number in [0,1] estimating how likely the person's gaze target lies within the current image area.
- **gaze\_point**: the (x,y) image coordinates of the person's point of attention (that is their gaze point). The origin (0,0) corresponds to the top-left corner. x increases to the right, y increases downward.

```
Note that you must always provide a gaze point, even if you believe the person is looking outside the image.
```

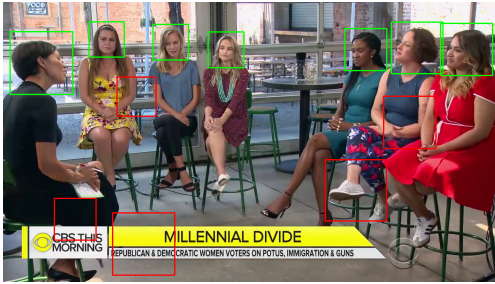
```
The person of interest is identified by the bounding box coordinates of their head in the user's input.
```

### J.1 PRBASE

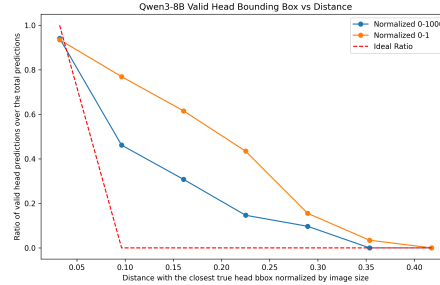
```
<Task description>
```

```
### Input/Output Format:
```

- **Input**: An image followed by a set of **bounding box coordinates** of the head of the person of interest.
- **Output**: Report in JSON format:
  - **inout**: the probability of looking inside the frame;



(a) Examples of positive (green) and negative (blue) head bounding boxes generated from the VAT test set. Negative boxes are constrained to have no overlap with any annotated head.



(b) Analysis of positive prediction given bounding box distance to the closest ground truth. Positive boxes have a distance of 0 and negative > 0.

```

- gaze_point the estimated gaze point coordinates.

Required Output Format:
### Gaze Point ###
```json
[
{"inout": <0.0-1.0>,"gaze_point": [x, y]}
]
```

```

## J.2 PRCOTBASE

```

<Task description>

In order to achieve your task, you can first do a step-by-step analysis.

Input/Output Format:
- Input: An image followed by a set of bounding box coordinates of the head of the person of interest.
- Output: Report in JSON format:
  - inout: the probability of looking inside the frame;
  - gaze_point the estimated gaze point coordinates.

Required Output Format:
### Reasoning ###
<Your step-by-step reasoning here>

### Gaze Point ###
```json
[
{"inout": <0.0-1.0>, "gaze_point": [x, y]}
]
```

```

### J.3 PRCOTSTRUCT

<Task description>

**\*\*In order to achieve your task, you can first do a step-by-step analysis\*\*.** Your entire response, including reasoning and final answer, must not exceed 1000 tokens and avoid repetition.

For instance, you can do the following:

1. Describe what is happening in the image.
2. Identify the activity or activities in which the person of interest is engaged in.
3. Determine the direction of gaze of the person of interest. Analyze the orientation of their head and eyes (if visible) to infer their gaze direction.
4. Identify and locate all plausible gaze targets (objects and/or persons) in the image that are visible to the person of interest, that is, that are within their field-of-view. Evaluate as well whether the person of interest is looking at something that is within the image area, or outside the image area.
5. Describe the spatial relationships between the person of interest and each of these plausible gaze targets.
6. Based on the scene context and information above, estimate how possible the person of interest is looking inside the frame and which plausible gaze target is the person of interest most likely looking at regardless of whether it is inside or outside the frame.
7. Using your reasoning, localize the most probable target of attention of the person of interest as a point. Use this point as the final gaze point. Provide the requested outputs (inout and gaze\_point).

### Input/Output Format:

- **\*\*Input:\*\*** An image followed by a set of **\*\*bounding box coordinates\*\*** of the head of the person of interest.
- **\*\*Output:\*\*** Report in JSON format:
  - **\*\*inout\*\***: the probability of looking inside the frame;
  - **\*\*gaze\_point\*\*** the estimated gaze point coordinates.

**\*\*Required Output Format:\*\***

### Reasoning ###

<Your step-by-step reasoning here>

### Gaze Point ###

```
```json
[
{"inout": <0.0-1.0>, "gaze_point": [x, y]}
]
```
```

### J.4 PRINCONTEXT-COT

<Task description>

**\*\*In order to achieve your task, you can first do a step-by-step analysis.\*\*** Your entire response, including reasoning and final answer, must not exceed 1000 tokens and avoid repetition.

```
### Input/Output Format:
- Input: An image followed by a set of bounding box coordinates
of the head of the person of interest.
- Output: Report in JSON format:
  - inout: the probability of looking inside the frame;
  - gaze_point the estimated gaze point coordinates.
```

```
Required Output Format:
### Reasoning ###
<Your step-by-step reasoning here>
```

```
### Gaze Point ###
```json
[
{"inout": <0.0-1.0>, "gaze_point": [x, y]}
]
```
```

To help you understand how to do the analysis, I provide you with two examples:

```
user:
<image>[0.0, 0.013, 0.279, 0.475]
```

```
assistant:
### Reasoning ###
1. The image shows a café or casual dining setting with two people sitting at a table. The person of interest is the woman on the left, identified by the provided head bounding box.
2. Her head and upper body are turned toward the right side of the image, which indicates that her attention is directed toward the man beside her or toward an object near him.
3. Her visible facial orientation suggests a rightward gaze rather than a downward look at the table or an upward look toward the background shelves. This makes the interaction area on the right side of the image the most likely region of attention.
4. Within that rightward region, the most plausible gaze targets are the man's face and the large white cup he is holding. The cup is the stronger candidate because it is visually salient, close to her line of sight, and central to the man's ongoing action, while his face is partly occluded by the cup. By contrast, other objects such as the glass on the table or the background shelves are less likely because they are either lower than her apparent line of sight or less relevant to the immediate interaction.
5. Therefore, the most likely gaze target is the large white cup on the right side of the image. Since this target is clearly inside the frame, the probability of looking inside the image should be high.
```

```
### Gaze Point ###
```json
[
{"inout": 1.0, "gaze_point": [0.81, 0.24]}
]
```
```

```
user:
<image>[0.333, 0.056, 0.498, 0.221]
```

```

assistant:
### Reasoning ###
1. The image shows a field sport scene with several players. The person
of interest is the player in red at the center, identified by the given
head bounding box.
2. His body is moving forward, but his head is turned toward the left
side of the image. His face orientation suggests that his attention is
not on the ground directly below him or on the distant players in the
background.
3. The most visually salient object in the direction of his head and
eyes is the small ball on the left side of the image. It is close to
him, in front of his hurley, and consistent with the ongoing action.
4. Other possible targets, such as the nearby teammate behind him or the
player in blue on the right, are less likely because they are not
aligned with his apparent line of sight. The ball is much more
consistent with both the sports context and his immediate action.
5. The ball is clearly inside the frame, so the probability that he is
looking inside the image is very high.
6. Therefore, the most plausible gaze target is the ball on the left
side of the image, with the gaze point placed near its center.

### Gaze Point ###
```json
[
{"inout": 1.0, "gaze_point": [0.14, 0.23]}
]
```

```

Example provided. Now, analyze the following image.

## K Zero-Shot Prompts for SG

For simplicity, we use <Task description> to denote the description of the social gaze prediction task.

For LAEO:

```

You are a helpful assistant specializing in human gaze analysis.
Your task is to analyze an input image, and determine whether the
people of interest are looking at each other.

```

```

The people of interest are identified by the bounding box
coordinates of their heads in the user's input.

```

For LAH:

```

You are a helpful assistant specializing in human gaze analysis.
Your task is to analyze an input image, and determine whether person A
is looking at person B.

```

```

The people of interest are identified by the bounding box
coordinates of their heads in the user's input.

```

For SA:

You are a helpful assistant specializing in **human gaze analysis**. Your task is to analyze an input image, and determine **whether the people of interest are sharing attention, i.e., looking towards the same object or person in the scene**.

The people of interest are identified by the **bounding box coordinates** of their heads in the user's input.

In addition, we use `<task>` to denote the social gaze task.

For LAEO:

looking at each other

For LAH:

person A looking at person B

For SA:

shared attention

## K.1 PRBASE

`<Task description>`

**### Input/Output Format:**

- **Input:** An image followed by a pair of **bounding box coordinates** of the heads of the people of interest.
- **Output:** Report in JSON format:
  - **label** the probability of `<task>`.

**Required Output Format:**

**### Social Gaze Label ###**

```
```json
[
  {"label": <0.0-1.0>}
]
```
```

## K.2 PRCOTBASE

`<Task description>`

**In order to achieve your task, you can first do a step-by-step analysis**.

**### Input/Output Format:**

- **Input:** An image followed by a pair of **bounding box coordinates** of the heads of the people of interest.
- **Output:** Report in JSON format:
  - **label** the probability of `<task>`.

```

**Required Output Format:**
### Reasoning ###
<Your step-by-step reasoning here>

### Social Gaze Label ###
```json
[
{"label": <0.0-1.0>}
]
```

```

### K.3 PRCOTSTRUCT

```

<Task description>

**In order to achieve your task, you can first do a step-by-step
analysis**. For instance, you can do the following:

1. Describe what is happening in the image.
2. Identify the activity or activities in which the people of interest
are engaged in.
3. Determine the direction of gaze of the people of interest. Analyze
the orientation of their head and eyes (if visible) to infer their gaze
direction.
4. Identify and locate all plausible gaze targets (objects and/or
persons) in the image that are visible to the people of interest, that
is, that are within their field-of-view.
5. Describe the spatial relationships between the people of interest and
each of these plausible gaze targets.
6. Based on the scene context and information above, determine whether
the people of interest are engaged in social gaze.
7. Using your reasoning, estimate the probability of <task> for the
people of interest.

### Input/Output Format:
- **Input:** An image followed by a pair of **bounding box coordinates**
of the heads of the people of interest.
- **Output:** Report in JSON format:
  - **label** the probability of <task>.

**Required Output Format:**
### Reasoning ###
<Your step-by-step reasoning here>

### Social Gaze Label ###
```json
[
{"label": <0.0-1.0>}
]
```

```

### K.4 PRINCONTEXT-COT

We provide the in-context prompt for VAT LAEO as an example. The in-context prompts for the other tasks and datasets follow the same format, and are available in the codebase.

<Task description>

**\*\*In order to achieve your task, you can first do a step-by-step analysis\*\***. Your entire response, including reasoning and final answer, must not exceed 1000 tokens and avoid repetition.

### Input/Output Format:

- **\*\*Input:\*\*** An image followed by a pair of **\*\*bounding box coordinates\*\*** of the heads of the people of interest.
- **\*\*Output:\*\*** Report in JSON format:
  - **\*\*label\*\*** the probability of looking at each other.

**\*\*Required Output Format:\*\***

### Reasoning ###

<Your step-by-step reasoning here>

### Social Gaze Label ###

```
```json
[
{"label": <0.0-1.0>}
]
```
```

To help you understand how to do the analysis, I provide you with two examples:

user:

<image> Analyze the image and determine whether the people with head boxes at [0.313, 0.421, 0.417, 0.606] and [0.443, 0.185, 0.570, 0.410] are looking at each other.

assistant:

### Reasoning ###

1. The two people are a woman in the center and a child to her lower left, sitting together on a bed with others around them.
2. They appear to be interacting in a group conversation or family scene.
3. The child's head is tilted upward toward the woman, so the child is looking at the woman's face/head.
4. The woman's head is turned slightly down and left toward the child, indicating her gaze is directed at the child.
5. Other plausible gaze targets exist in the room, but both people's faces are oriented toward each other more than toward anyone else.
6. So the people are looking at each other.

### Social Gaze Label ###

```
```json
[
{"label": 1}
]
```
```

user:

<image> Analyze the image and determine whether the people with head boxes at [0.330, 0.210, 0.407, 0.348] and [0.427, 0.294, 0.527, 0.470] are looking at each other.

assistant:

### ### Reasoning ###

1. The two people are soldiers seated among others while handling gear on the ground.
2. The scene is a busy military prep area, and both appear focused on equipment rather than on each other.
3. The left soldier has head angled downward and slightly right, toward the items in front of him.
4. The right soldier also has head angled downward, looking at the gear or his hands.
5. Although they are near each other, their gaze directions do not align with each other's heads.
6. So they are not looking at each other.

### ### Social Gaze Label ###

```
```json
[
  {"label": 0}
]
```
```

Examples provided. Now, analyze the following image.

## L Question Templates in QA Pair Construction

### Gaze Following In/Out Questions

- “Is the gaze target of <OnePerson> inside the frame?”
- “Is <OnePerson> looking at something in the scene?”
- “What is the probability that the focus of <OnePerson> lies inside the current image area?”
- “How probable is it that <OnePerson> is looking at something within the boundaries of the scene?”
- “How certain are you that what <OnePerson> is looking at is shown in the image?”
- “Estimate the probability that the gaze point of <OnePerson> lies within the frame.”
- “Rate the likelihood that the gaze of <OnePerson> is directed at something within the frame.”
- “Assign a probability representing the chance that the visual target of <OnePerson> lies inside the frame.”
- “Determine the probability that the focus of <OnePerson> is contained within the scene.”
- “Evaluate the chance that <OnePerson> is looking at something that is in this photograph.”

### Gaze Following Gaze Point Questions

- “Where is <OnePerson> looking?”
- “What is the gaze point of <OnePerson>?”
- “Where is the focus of <OnePerson>?”
- “Estimate the gaze point of <OnePerson>.”
- “Localize the gaze point of <OnePerson> within the image.”
- “Where is the visual target of <OnePerson> in the image?”
- “Where is the attention of <OnePerson> currently directed?”

- “Find the point of interest for <OnePerson>.”
- “Determine the gaze destination of <OnePerson>.”
- “What are the coordinates of the gaze target for <OnePerson> within the frame?”

#### LAEO Questions

- “Are the <TwoPersons> in the image looking at each other?”
- “Is there eye contact between the <TwoPersons>?”
- “There are <TwoPersons> in the image. Do these two people appear to be making eye contact?”
- “We can see <TwoPersons> in the image. Are their gazes directed toward one another?”
- “Are the <TwoPersons> mutually looking at each other?”
- “Estimate the probability that the <TwoPersons> are engaged in eye contact.”
- “What is the chance that <OnePerson> and <OnePerson> are looking at each other?”
- “Is there eye contact between <OnePerson> and <OnePerson>?”
- “Do the <TwoPersons> appear to be looking at each other?”
- “Would you say the <TwoPersons> are making eye contact?”

#### LAH Questions

- “Is <OnePerson> looking at <OnePerson>?”
- “There are <TwoPersons> in the image. Does <OnePerson> appear to be looking at <OnePerson>?”
- “We can see <TwoPersons> in the image. Is <OnePerson> looking at <OnePerson>?”
- “Estimate the probability that <OnePerson> is looking at <OnePerson>?”
- “What is the chance that <OnePerson> is looking at <OnePerson>?”
- “Does <OnePerson> seem to be looking toward <OnePerson>?”
- “How likely is it that <OnePerson> is looking at <OnePerson>?”
- “Give a probability that <OnePerson> is looking at <OnePerson>.”
- “There are <TwoPersons> visible in the image. Does <OnePerson> seem to be looking at <OnePerson>?”
- “Would you say <OnePerson> is looking at <OnePerson>?”

#### SA Questions

Same format as LAEO questions, replace “eye contact” and “looking at each other” with “sharing attention” to get the questions.

#### <OnePerson>

- “the <person> whose head is within the bounding box  $[x_{\min}, y_{\min}, x_{\max}, y_{\max}]$ ”
- “the <person> located at  $[x_{\min}, y_{\min}, x_{\max}, y_{\max}]$ ”
- “the <person> whose head is enclosed by the bounding box  $[x_{\min}, y_{\min}, x_{\max}, y_{\max}]$ ”
- “the <person> whose head is bounded by  $[x_{\min}, y_{\min}, x_{\max}, y_{\max}]$ ”
- “the <person> whose head is identified in the region  $[x_{\min}, y_{\min}, x_{\max}, y_{\max}]$ ”

#### <TwoPerson>

- “the <persons> whose heads are within the bounding boxes  $[x_{\min}^{(1)}, y_{\min}^{(1)}, x_{\max}^{(1)}, y_{\max}^{(1)}]$  and  $[x_{\min}^{(2)}, y_{\min}^{(2)}, x_{\max}^{(2)}, y_{\max}^{(2)}]$ ”
- “the <persons> located at  $[x_{\min}^{(1)}, y_{\min}^{(1)}, x_{\max}^{(1)}, y_{\max}^{(1)}]$  and  $[x_{\min}^{(2)}, y_{\min}^{(2)}, x_{\max}^{(2)}, y_{\max}^{(2)}]$ ”
- “the <persons> whose heads are enclosed by the bounding boxes  $[x_{\min}^{(1)}, y_{\min}^{(1)}, x_{\max}^{(1)}, y_{\max}^{(1)}]$  and  $[x_{\min}^{(2)}, y_{\min}^{(2)}, x_{\max}^{(2)}, y_{\max}^{(2)}]$ ”

- "the <persons> whose heads are bounded by  $[x_{\min}^{(1)}, y_{\min}^{(1)}, x_{\max}^{(1)}, y_{\max}^{(1)}]$  and  $[x_{\min}^{(2)}, y_{\min}^{(2)}, x_{\max}^{(2)}, y_{\max}^{(2)}]$ "
- "the <persons> whose heads are identified in the regions  $[x_{\min}^{(1)}, y_{\min}^{(1)}, x_{\max}^{(1)}, y_{\max}^{(1)}]$  and  $[x_{\min}^{(2)}, y_{\min}^{(2)}, x_{\max}^{(2)}, y_{\max}^{(2)}]$ "

<person> = person | subject | individual | human

<persons> = people | subjects | individuals | humans

## M Limitations

This work has a few limitations. First, due to the construction of VSGaze, the shared attention annotations in VAT and ChildPlay are limited to attention shared toward human heads. As a result, our benchmark does not yet evaluate shared attention toward objects or other scene entities. Extending the annotation space to include object-level and more general scene-level shared attention would provide a more comprehensive evaluation of social gaze understanding.

Second, although VLMs approach the performance of MTGS [10] on social gaze, it is important to note that MTGS is trained on VSGaze, whose data distribution differs from the sampled social gaze data used in this work. VSGaze incorporates additional datasets, including VideoCoAtt [8] and UCO-LAEO [24], and contains substantially more negative pairs. The original paper finds that this broader training setup introduces additional challenges and can lead to underperformance relative to dataset-specific training, which enables models to learn dataset-specific priors.

Third, VLMs are substantially larger than specialized gaze models, which leads to higher hardware requirements during both fine-tuning and inference, especially in terms of GPU memory. Their autoregressive next-token prediction mechanism also makes inference slower than direct prediction models, and this cost becomes more pronounced when using thinking or reasoning modes, where a complete prediction may take several seconds. A promising direction is therefore to design more efficient architectures that better exploit VLM features while reducing the computational overhead for gaze-specific prediction.

Fourth, when fine-tuning VLMs for gaze following and social gaze prediction, the supervision is applied through text-based language modeling losses rather than direct numerical losses on gaze coordinates or social gaze labels. This makes the optimization objective less directly aligned with the target evaluation metrics than in specialized gaze models. Whether language-modeling-based optimization can provide gradients that are sufficiently consistent with task-specific spatial and semantic objectives remains an important question for future research.

Finally, evaluating closed-source VLMs at scale is costly because inference requires paid API calls, and the strongest models are often expensive to query. Therefore, we evaluate closed-source models on 1k subsets for each task. Although this setting provides a practical comparison under realistic budget constraints, larger-scale evaluation would yield more robust and comprehensive estimates of their gaze understanding performance.

## N Broader Impact

Understanding human gaze behavior has several positive societal applications, including the development of automated tools to support clinicians in tasks such as autism screening [49, 50], where gaze patterns can provide important diagnostic cues. Because VLMs often offer easy-to-use interfaces, our study can help practitioners better understand the capabilities and limitations of current models when applied to gaze-related tasks.

At the same time, the increasing accessibility of such tools raises important ethical considerations. Gaze data can reveal sensitive information about attention, preferences, health, and cognitive state, creating risks related to privacy, surveillance, and misuse. These tools should therefore only be used only in appropriate contexts, and with the prior informed consent of the individuals being observed.